LOW COMPLEXITY EQUALIZATION FOR AFDM IN DOUBLY DISPERSIVE CHANNELS

Ali Bemani[1], Nassar Ksairi[2], Marios Kountouris[1]

[1] Communication Systems Department, EURECOM, Sophia Antipolis, France
[2] Mathematical and Algorithmic Sciences Lab, Huawei France R&D, Paris, France
Email: ali.bemani@eurecom.fr, nassar.ksairi@huawei.com, marios.kountouris@eurecom.fr

ABSTRACT

Affine Frequency Division Multiplexing (AFDM), which is based on discrete affine Fourier transform (DAFT), has recently been proposed for reliable communication in high-mobility scenarios. Two low complexity detectors for AFDM are introduced here. Approximating the channel matrix as a band matrix via placing null symbols in the AFDM frame in the DAFT domain, a low complexity MMSE detection is proposed by means of the LDL factorization. Furthermore, exploiting the sparsity of the channel matrix, we propose a low complexity iterative decision feedback equalizer (DFE) based on weighted maximal ratio combining (MRC), which extracts and combines the received multipath components of the transmitted symbols in the DAFT domain. Simulation results show that the proposed detectors have similar performance, while weighted MRC-based DFE has lower complexity than band-matrix-approximation LMMSE when the channel impulse response has gaps.

Index Terms— AFDM, affine Fourier transform, doubly dispersive channels, detector, MMSE, DFE, MRC.

1. INTRODUCTION

Next-generation wireless systems (e.g., B5G/6G) are evolving to cater to a wide range of applications and services requiring reliable communication in high-mobility scenarios. This calls for new waveform design able to cope with time-varying channels. In this setting, existing waveforms, in particular orthogonal frequency division multiplexing (OFDM), lose subcarrier orthogonality, thus resulting in inter-carrier interference and deteriorated system performance.

Affine frequency division multiplexing (AFDM) has recently been proposed as a promising waveform for communication in time-varying channels [1, 2] showing significant performance gains over OFDM. AFDM employs multiple orthogonal information-bearing chirps generated using the discrete affine Fourier transform (DAFT). A key feature is that its chirp pulse parameters can be adapted to the channel characteristics, making a complete delay-Doppler representation of the channel in the DAFT domain. This enables AFDM

to achieve full diversity in doubly dispersive channels [1] as opposed to existing chirp-based waveforms, for instance [3, 4]. Furthermore, AFDM has similar performance in terms of bit error rate (BER) with orthogonal time frequency space (OTFS) [5]. However, AFDM outperforms OTFS in terms of pilot overhead and multiuser multiplexing overhead [2, 6].

In this paper, we propose two low complexity detection algorithms for AFDM taking advantage of its inherent channel sparsity. By placing some null symbols - zero padding the AFDM frame - in the DAFT domain, the channel matrix can be approximated as a band matrix. Using the approximated band matrix and inspired by the equalizer in [7] for OFDM systems, we first design a low complexity MMSE detector based on LDL factorization [8]. The overall complexity of the proposed algorithm is linear in the number of subcarriers and quadratic in the bandwidth of the band matrix, which in turn depends on the the maximum delay and maximum Doppler shift. Second, we propose a low complexity iterative decision feedback equalizer (DFE) based on weighted maximal ratio combining (MRC) of the channel impaired input symbols received from different paths. The overall complexity of the second algorithm is also linear in the number of subcarriers and quadratic in the number of paths. We show that these two detectors have similar performance, whereas when the channel is sparse in the delay domain, weighted MRC-based DFE detector exhibits lower complexity.

2. SYSTEM MODEL

The AFDM block diagram is given in Fig. 1. Modulation is produced by using DAFT at the transmitter and receiver. DAFT is a discretized version of AFT [1, 9–11] and its kernel is equal to $e^{-\imath 2\pi(c_2 m^2 + \frac{1}{N} mn + c_1 n^2)}$ where c_1 and c_2 are the AFDM parameters tuned to provide full delay-Doppler representation of the channel in the DAFT domain. It has been shown that tuning c_1 using the the maximum Doppler shift normalized with respect to the subcarrier spacing, and setting c_2 to be an arbitrary irrational number or a rational number sufficiently smaller than $1/2N$, enables AFDM to achieve full diversity in doubly dispersive channels [1].

2.1. Modulation and Demodulation

Consider a set of quadrature amplitude modulation (QAM) symbols $x_k, k = 0, 1, 2, ..., N - 1$. AFDM maps x_k to s_n
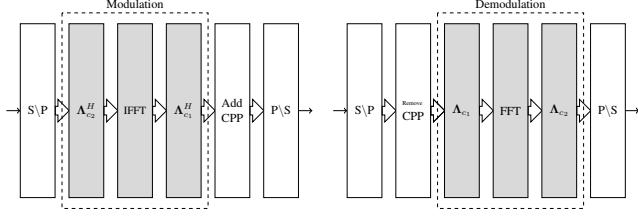
Fig. 1: AFDM modulation/demodulation block diagram.

using inverse DAFT (IDAFT) as follows:

$$s_n = \frac{1}{\sqrt{N}} \sum_{m=0}^{N-1} x_m e^{i2\pi(c_2 m^2 + \frac{1}{N}mn + c_1 n^2)}, \quad n = 0, \cdots, N-1. \tag{1}$$

To make the channel lie in a periodic domain, a *chirp-periodic prefix* (CPP) should be added to the modulated signal, defined as

$$s_n = s_{N+n} e^{-i2\pi c_1(N^2 + 2Nn)}, \quad n = -M, \cdots, -1 \tag{2}$$

where M is any integer greater than or equal to the value in samples of the maximum delay spread of the wireless channel. After transmission over the channel, the received samples are

$$r_n = \sum_{l=0}^{\infty} s_{n-l} g_n(l) + w_n \tag{3}$$

where $w_n \sim \mathcal{CN}(0, N_0)$ is an additive Gaussian noise and $g_n(l)$ is the impulse response of the time-varying channel at time n and delay l, given by

$$g_n(l) = \sum_{i=1}^{P} h_i e^{-i2\pi f_i n} \delta(l - l_i) \tag{4}$$

where $P \geq 1$ is the number of paths, $\delta(\cdot)$ is the Dirac delta function, and h_i, f_i and l_i are the complex gain, Doppler shift (in digital frequencies), and the integer delay associated with the i-th path, respectively. We define $\nu_i \triangleq N f_i$, where $\nu_i \in [-\nu_{\max}, \nu_{\max}]$ is the Doppler shift normalized with respect to the subcarrier spacing. We assume that the maximum delay of the channel satisfies $l_{\max} \triangleq \max(l_i) < N$.
The DAFT domain output symbols are obtained by

$$y_m = \frac{1}{N} \sum_{n=0}^{N-1} r_n e^{-i2\pi(c_2 m^2 + \frac{1}{N}mn + c_1 n^2)}. \tag{5}$$

Discarding the CPP, the input-output relation can be written in matrix form as

$$\mathbf{y} = \mathbf{A}\mathbf{r} = \mathbf{H}_{\text{eff}}\mathbf{x} + \mathbf{A}\mathbf{w} \tag{6}$$

where $\mathbf{A} = \mathbf{\Lambda}_{c_2}\mathbf{F}\mathbf{\Lambda}_{c_1}$ is the DAFT matrix, $\mathbf{F}$ is the discrete Fourier transform (DFT) matrix with entries $e^{-i2\pi mn/N}/\sqrt{N}$, $\mathbf{\Lambda}_c = \text{diag}(e^{-i2\pi cn^2}, n = 0, 1, \ldots, N-1)$, $\mathbf{H}_{\text{eff}} = \mathbf{A}\mathbf{H}\mathbf{A}^{\text{H}}$, and $\mathbf{H}$ is the matrix representation of the channel. The elements of $\mathbf{y}$, $\mathbf{r}$, $\mathbf{x}$ and $\mathbf{w} \sim \mathcal{CN}(\mathbf{0}, \mathbf{N_0 I})$ are similarly related to y_k, r_k, x_k and w_k, respectively. Since $\mathbf{A}$ is a unitary matrix, $\widetilde{\mathbf{w}} = \mathbf{A}\mathbf{w}$ and $\mathbf{w}$ have the same statistics. $\mathbf{H}_{\text{eff}}$ has
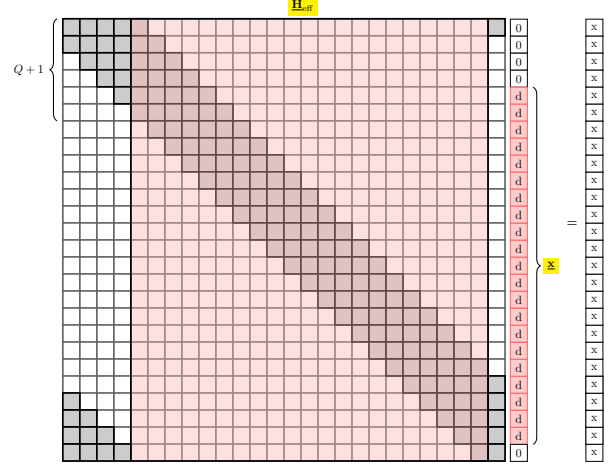

Fig. 2: Truncated parts of $\mathbf{x}$ and $\mathbf{H}_{\text{eff}}$

sparse structure i.e., there are exactly $L = P$ non-zero entries in each row and column if ν_i is integer and if we set $c_1 = \frac{2\nu_{\max}+1}{2N}$. Indeed, in this case $\mathbf{H}_{\text{eff}} = \sum_{i=1}^{P} h_i \mathbf{H}_i$ where

$$\mathbf{H}_i(p, q) = \begin{cases} e^{i\frac{2\pi}{N}(Nc_1 l_i^2 - ql_i + Nc_2(q^2 - p^2))} & q = (p + \text{loc}_i)_N \\ 0 & \text{otherwise} \end{cases} \tag{7}$$

where $\text{loc}_i = (\nu_i + (2\nu_{\max} + 1)l_i)_N$ [1]. For fractional ν_i, it can be shown that $\mathbf{H}_i$ has in each row and column a peak surrounded by approximately $2k_\nu$ non-zero entries decreasing rapidly as we move away from it. Hence, if we set $c_1 = \frac{2(\lfloor \nu_{\max} \rfloor + k_\nu) + 1}{2N}$, $\mathbf{H}_{\text{eff}}$ can be approximated as having $L = (2k_\nu + 1)P$ non-zero entries per row and column (i.e., each received symbol can be approximately expressed as a linear combination of only a few input symbols). We propose below two low complexity detection algorithms leveraging the channel matrix sparsity.

3. DETECTION ALGORITHMS

The first step is to place some null symbols that allow to approximate the truncated part of $\mathbf{H}_{\text{eff}}$ as a band matrix. This also simplifies the input-output relation as the modular operation is no longer needed, as shown in Fig. 2. Note that these symbols do not entail extra overhead as they can serve not only the proposed detection algorithms but also embedded pilot aided channel estimation. Due to the structure of $\mathbf{H}_{\text{eff}}$ and $\mathbf{H}_i$, the number of the null guard symbols should be greater than $Q = (l_{\max} + 1)(2(\alpha_{\max} + k_\nu) + 1) - 1$. Taking into account the zero padding, the vector of DAFT domain received samples writes as

$$\mathbf{y} = \underline{\mathbf{H}}_{\text{eff}}\underline{\mathbf{x}} + \widetilde{\underline{\mathbf{w}}} \tag{8}$$

where $\underline{\mathbf{x}}$ and $\underline{\mathbf{H}}_{\text{eff}}$ are the truncated parts of $\mathbf{x}$ and $\mathbf{H}_{\text{eff}}$, respectively (see Fig. 2). They can be expressed using the matrix $\mathbf{T} = [\mathbf{I}_N]_{Q-(\alpha_{\max}+k_\nu):N-(\alpha_{\max}+k_\nu)-1,:}$ as $\underline{\mathbf{x}} = \mathbf{T}\mathbf{x}$ and $\underline{\mathbf{H}}_{\text{eff}} = \mathbf{H}_{\text{eff}}\mathbf{T}^{\text{H}}$. Using LMMSE equalization based on (8) for detection requires $\mathcal{O}(N^3)$ flops, which can be prohibitive

for large N. We thus propose two detectors with lower complexity. The first is a low-complexity LMMSE based on a band approximation of $\underline{\mathbf{H}}_{\text{eff}}$. The second is a weighted MRC-based DFE exploiting the sparse representation of the communication channel provided by AFDM.

3.1. Low complexity MMSE detection

To recover the data symbols $\underline{\mathbf{x}}$, considering (8), the following MMSE equalization is used

$$\hat{\underline{\mathbf{x}}} = \underline{\mathbf{H}}_{\text{eff}}^{\text{H}}(\underline{\mathbf{H}}_{\text{eff}}\underline{\mathbf{H}}_{\text{eff}}^{\text{H}} + N_0\mathbf{I}_N)^{-1}\mathbf{y}. \tag{9}$$

Although (9) involves matrix inversion, the matrix $\mathbf{M} = \underline{\mathbf{H}}_{\text{eff}}\underline{\mathbf{H}}_{\text{eff}}^{\text{H}} + N_0\mathbf{I}_N$ is a Hermitian band matrix with lower and upper bandwidth Q. Thus, $\mathbf{M}^{-1}$ can be computed using LDL factorization. Algorithm 1 can be performed to efficiently equalize the received signal. The computational

---

Algorithm 1: Low complexity MMSE detection

1 Construct the matrix $\underline{\mathbf{H}}_{\text{eff}} = \mathbf{H}_{\text{eff}}\mathbf{T}^{\text{H}}$
2 Construct the band matrix $\mathbf{M} = \underline{\mathbf{H}}_{\text{eff}}\underline{\mathbf{H}}_{\text{eff}}^{\text{H}} + N_0\mathbf{I}_N$
3 Compute the LDL factorization of $\mathbf{M} = \mathbf{LDL}^{\text{H}}$
  where $\mathbf{L}$ is a lower triangular matrix with Q sub diagonals and $\mathbf{D}$ is a diagonal matrix
4 Solve the triangular system $\mathbf{Lf} = \mathbf{y}$
5 Solve the diagonal system $\mathbf{Dg} = \mathbf{f}$
6 Solve the triangular system $\mathbf{L}^{\text{H}}\mathbf{d} = \mathbf{g}$
7 Calculate $\hat{\underline{\mathbf{x}}} = \underline{\mathbf{H}}_{\text{eff}}^{\text{H}}\mathbf{d}$

---

cost of the proposed detection algorithm is evaluated in terms of complex additions (CAs), complex multiplications (CMs) and complex divisions (CDs). The first step does not need any complex operation since $\underline{\mathbf{H}}_{\text{eff}}$ is truncated from $\mathbf{H}_{\text{eff}}$. In step 2, every element of $\underline{\mathbf{H}}_{\text{eff}}\underline{\mathbf{H}}_{\text{eff}}^{\text{H}}$ requires at most $Q+1$ CMs and Q CAs. Considering that $\underline{\mathbf{H}}_{\text{eff}}\underline{\mathbf{H}}_{\text{eff}}^{\text{H}}$ is Hermitian and neglecting some small terms in the complexity expression, step 2 requires $\frac{1}{2}(Q^2+3Q+2)N$ CMs and $\frac{1}{2}(Q^2+Q+2)N$ CAs. Similar to [7], step 3, the LDL factorization, requires $\frac{1}{2}(Q^2+3Q)N$ CMs, $\frac{1}{2}(Q^2+Q)N$ CAs, and QN CDs. Steps 4 and 6 can be solved by band forward and backward substitutions [8] and each of them has QN CMs and QN CAs. Step 5 can be solved using N CDs since $\mathbf{D}$ is a diagonal matrix and the last step requires $(Q+1)N$ CMs and QN CAs. Thus, the algorithm requires $(Q^2+6Q+2)N$ CMs, $(Q^2+4Q+1)N$ CAs and $(Q+1)N$ CDs, which amounts to $(2Q^2+11Q+4)N$ complex operations in total.

3.2. Weighted MRC-based DFE detection

As mentioned in Section 2, $\underline{\mathbf{H}}_{\text{eff}}$ has L non-zero entries per column. This feature enables us to propose a weighted MRC-based detector where each data symbol is detected from the weighted MRC of its L channel-impaired received copies. Fig. 3 shows an example of this detector for AFDM with $N = 8$ and a 3-path channel with $Q = 2$. The proposed detector is iterative, where in each iteration, the estimated inter symbol interference is canceled in the branches selected
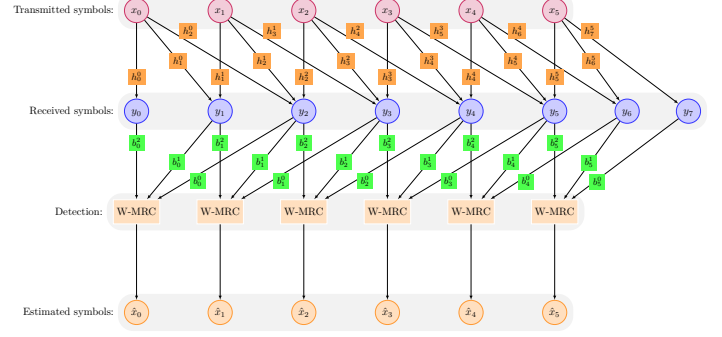

Fig. 3: Weighted MRC operation for $N = 8$ with a 3-path channel with $Q = 2$ where W-MRC stands for weighted MRC and $h_i^j = \underline{\mathbf{H}}_{\text{eff}}(i, j)$.

for the combining. Considering the structure of $\underline{\mathbf{H}}_{\text{eff}}$, it can be seen that each received symbol y_k is given by

$$y_k = \sum_{i=0}^{L-1} \underline{\mathbf{H}}_{\text{eff}}(k, p_k^i)x_{p_k^i} \tag{10}$$

where p_k^i is the column index of the i-th path coefficient in row k of matrix $\underline{\mathbf{H}}_{\text{eff}}$. Let b_k^i be the channel impaired input symbol x_k in the received samples $y_{q_k^i}$ after canceling the interference from other input symbols, where q_k^i is the row index of the i-th path coefficient in column k of matrix $\underline{\mathbf{H}}_{\text{eff}}$. In each iteration, assuming estimates of the input symbols x_k are available either from the current iteration (for $p_{q_k^i}^j < k, \quad j = 0, ..., L-1$) or previous iteration (for $p_{q_k^i}^j > k, \quad j = 0, ..., L-1$), b_k^i can be written as

$$b_k^i = y_{q_k^i} - \sum_{p_{q_k^i}^j < k} \underline{\mathbf{H}}_{\text{eff}}^{\text{H}}(q_k^i, p_{q_k^i}^j)\hat{x}_{p_{q_k^i}^j}^{(n)} - \sum_{p_{q_k^i}^j > k} \underline{\mathbf{H}}_{\text{eff}}^{\text{H}}(q_k^i, p_{q_k^i}^j)\hat{x}_{p_{q_k^i}^j}^{(n-1)} \tag{11}$$

where superscript (n) denotes the n-th iteration. Considering b_k^i for all paths $i = 0, 1, ..., L-1$, weighted MRC (as opposed to pure MRC [12]) can be performed. The output of the weighted MRC for estimating x_k is given by

$$c_k = \frac{g_k}{d_k + \gamma^{-1}} \tag{12}$$

where

$$g_k \triangleq \sum_{i=0}^{L-1} \underline{\mathbf{H}}_{\text{eff}}^{\text{H}}(q_k^i, k)b_k^i, \tag{13}$$

$$d \triangleq \sum_{i=0}^{L-1} |\underline{\mathbf{H}}_{\text{eff}}^{\text{H}}(q_k^i, k)|^2 \tag{14}$$

and γ is the signal-to-noise ratio (SNR). Let $\mathcal{D}(.)$ denote the decision on the symbol estimate c_k, i.e, $\hat{x}_k^n = \mathcal{D}(c_k)$. In this paper, we consider $\hat{x}_k^n = c_k$. The estimated symbols are then

used for the next iteration. The algorithm continues until the maximum number of iterations is reached or the updated input symbol vector is close enough to the previous one as summarized in Algorithm 2.

Algorithm 2: Weighted MRC-based DFE detection

Data: $\underline{\mathbf{H}}_{\text{eff}}, d, \mathbf{y}, \hat{\mathbf{x}}^0 = \mathbf{0}$

1 **for** $n = 1 : n_{\text{iter}}$ **do**

2   **for** $k = 0 : N\text{-}Q\text{-}1$ **do**

3   **for** $i = 0 : L\text{-}1$ **do**

4 $b_k^i = y_{q_k^i} - \sum_{p_{q_k^i}^j < k} \underline{\mathbf{H}}_{\text{eff}}^{\text{H}}(q_k^i, p_{q_k^i}^j)\hat{x}_{p_{q_k^i}^j}^{(n)}$

          $- \sum_{p_{q_k^i}^j > k} \underline{\mathbf{H}}_{\text{eff}}^{\text{H}}(q_k^i, p_{q_k^i}^j)\hat{x}_{p_{q_k^i}^j}^{(n-1)}$

5   **end**

6 $g_k = \sum_{i=0}^{L-1} \underline{\mathbf{H}}_{\text{eff}}^{\text{H}}(q_k^i, k)b_k^i$

7 $c_k = \frac{g_k}{d_k + \gamma^{-1}}$

8 $\hat{x}_k^{(n)} = c_k$ or $\hat{x}_k^{(n)} = \mathcal{D}(c_k)$

9   **end**

10   **if** $||\hat{\mathbf{x}}^{(n)} - \hat{\mathbf{x}}^{(n-1)}|| < \epsilon$ **then** EXIT;

11 **end**

Computing the complexity of Algorithm 2 is straightforward as it has only scalar operation. From step 3 to step 11, it requires L^2 CMs, L^2 CAs and 1 CD. Therefore, its total complexity is $n_{\text{iter}}(2L^2+1)(N-Q)$. In simulations, we observed that the algorithm typically converges within 15 iterations. In the longer version of the article, convergence of $\hat{\mathbf{x}}^{(n)}$ to the LMMSE estimate $\hat{\underline{\mathbf{x}}}$ defined in (9) is proved.

The complexity of the two proposed algorithms is remarkably smaller than maximum likelihood (ML) and linear MMSE detectors, which have exponential $\mathcal{O}(|\mathbb{A}|^N)$ and cubic $\mathcal{O}(N^3)$ complexity, respectively, with $\mathbb{A}$ representing the QAM alphabet. Moreover, Algorithm 2 has lower complexity than Algorithm 1 when the channel impulse response has gaps. This is due to the fact that its complexity only depends on the number of non-zero elements in each column of $\underline{\mathbf{H}}_{\text{eff}}$, i.e L, instead of $Q \geq L$.

4. SIMULATION RESULTS

In this section, we simulate the uncoded BER performance of AFDM over doubly dispersive channels. The following parameters are used: carrier frequency $f_c = 4$ GHz, number of subcarriers $N = 128$, and AFDM frame length $330~\mu$s. Path delays are fixed, and considering Jakes Doppler spectrum for each channel realization, the Doppler shift of the i-th path is generated using $\nu_i = \nu_{\max} cos(\theta_i)$, where θ_i is uniformly distributed over $[-\pi, \pi]$ with 4-QAM signaling. The maximum Doppler shift is $\nu_{\max} = 1$, which corresponds to a maximum speed of 810 km/h. Fig. 4a shows the BER performance of AFDM using the proposed weighted MRC-based DFE detector for different values of ϵ at SNR = 20 dB. We can see that below $\epsilon = 0.01$, the performance remains almost
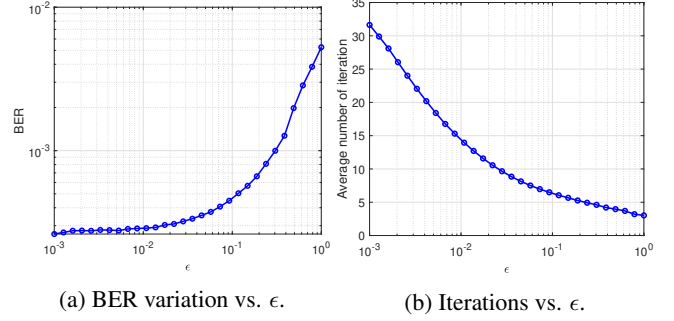

(a) BER variation vs. ϵ.   (b) Iterations vs. ϵ.

Fig. 4: BER variation and the average number of iterations versus ϵ for the weighted MRC-based DFE detector for 4-QAM, $N = 128$ and SNR = 20 dB.
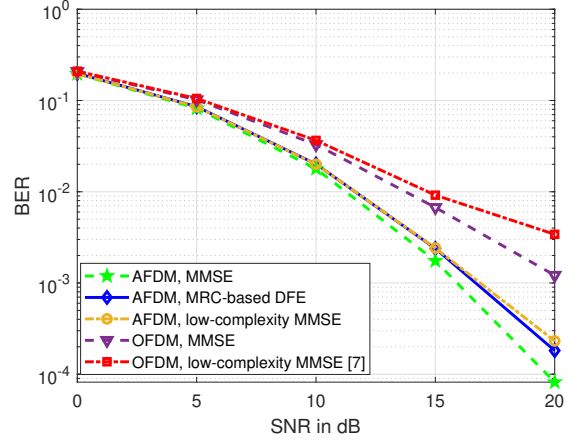

Fig. 5: BER performance comparison between AFDM and OFDM systems using different detectors

constant, and the algorithm converges within 14 iterations, as shown in Fig. 4b. In Fig. 5, we plot the BER performance of AFDM and OFDM for LMMSE, low-complexity MMSE [7] and weighted MRC-based DFE detectors. First, we observe that AFDM outperforms OFDM, thanks to achieving full diversity and as every information symbol is received through multiple independent non-overlapping paths. Second, we observe that both proposed detection algorithms have similar performance between them, while conventional MMSE detection has slightly better performance at the cost of higher complexity.

5. CONCLUSION

We proposed two low complexity detection algorithms for zero-padded AFDM. First, a low complexity MMSE detector which makes use of band LDL factorization was derived. Second, an iterative weighted MRC-based DFE detector, which exploits the channel sparsity, was proposed. Our results showed that both detectors have comparable performance as exact LMMSE while their complexity order is linear, instead of cubic, in the number of subcarriers.

6. REFERENCES

[1] A. Bemani, N. Ksairi, and M. Kountouris, "AFDM: A full diversity next generation waveform for high mobility communications," in *2021 IEEE International Conference on Communications Workshops (ICC Workshops)*, 2021, pp. 1–6.

[2] A. Bemani, G. Cuozzo, N. Ksairi, and M. Kountouris, "Affine frequency division multiplexing for next-generation wireless networks," in *2021 International Symposium on Wireless Communication Systems (ISWCS)*, 2021, pp. 1–6.

[3] R. Bomfin, M. Chafii, A. Nimr, and G. Fettweis, "A robust baseband transceiver design for doubly-dispersive channels," *IEEE Trans. on Wireless Communications*, vol. 20, no. 8, pp. 4781–4796, 2021.

[4] R. Bomfin, M. Chafii, and G. Fettweis, "Low-complexity iterative receiver for orthogonal chirp division multiplexing," in *2019 IEEE Wireless Communications and Networking Conference Workshop (WCNCW)*. IEEE, 2019, pp. 1–6.

[5] R. Hadani, S. Rakib, M. Tsatsanis, A. Monk, A. J. Goldsmith, A. F. Molisch, and R. Calderbank, "Orthogonal time frequency space modulation," in *IEEE Wireless Communications and Networking Conference (WCNC)*, 2017, pp. 1–6.

[6] P. Raviteja, K. T. Phan, and Y. Hong, "Embedded pilot-aided channel estimation for OTFS in delay–doppler channels," *IEEE Trans. on Vehicular Technology*, vol. 68, no. 5, pp. 4906–4917, 2019.

[7] L. Rugini, P. Banelli, and G. Leus, "Simple equalization of time-varying channels for OFDM," *IEEE communications letters*, vol. 9, no. 7, pp. 619–621, 2005.

[8] G. H. Golub and C. F. Van Loan, "Matrix computations," *Johns Hopkins University Press, 3rd edition*, 1996.

[9] J. J. Healy, M. A. Kutay, H. M. Ozaktas, and J. T. Sheridan, *Linear canonical transforms: Theory and applications*. Springer, 2015.

[10] S.-C. Pei and J.-J. Ding, "Relations between fractional operations and time-frequency distributions, and their applications," *IEEE Trans. on Signal Processing*, vol. 49, no. 8, pp. 1638–1655, 2001.

[11] S. Pei and J. Ding, "Closed-form discrete fractional and affine Fourier transforms," *IEEE Trans. on Signal Processing*, vol. 48, no. 5, pp. 1338–1353, 2000.

[12] T. Thaj and E. Viterbo, "Low complexity iterative rake decision feedback equalizer for zero-padded otfs systems," *IEEE Trans. on Vehicular Technology*, vol. 69, no. 12, pp. 15 606–15 622, 2020.